

# ARPES spectra and the single particle spectral weight of cuprates in the bond-ordered, bond-centered stripe phase

P. Wróbel<sup>1,2</sup>, A. Maciąg<sup>2</sup> and R. Eder<sup>3</sup>

<sup>1</sup> Max Planck Institute for the Physics of Complex Systems, D-01187 Dresden, Germany

<sup>2</sup> Institute for Low Temperature and Structure Research,

P. O. Box 1410, 50-950 Wrocław 2, Poland and

<sup>3</sup> Forschungszentrum Karlsruhe, IFP, P.O. Box 3640, D-76021 Karlsruhe, Germany

The electronic structure and the single-particle spectral density of a stripe array formed by ladder-like domain walls (DWs) and by antiferromagnetic (AF) domains of width 2 lattice spacings are computed and compared with ARPES spectra from some doped cuprates belonging to the 214 family of compounds. We assume that bond order is formed on legs in DWs and that the phase of the sublattice magnetization changes by  $\pi$  across each DW. The intensity map plotted in the coordination frame momentum-energy reproduces quite well the ARPES spectra obtained at the doping level of 15%. We consider this agreement as an argument for a scenario of coexisting bond-ordered regions and AF regions in the stripe phase of moderately doped cuprates.

PACS numbers: 71.10.Fd, 74.20.Mn, 74.72.-h, 79.60.-i

## I. INTRODUCTION

A tendency towards spin and charge ordering in cuprates has been observed in results of several neutron scattering experiments. Low frequency spin fluctuations observed by many groups at incommensurate wave vectors as relatively sharp peaks in the magnetic structure factor [1, 2, 3] have been interpreted as being due to stripe fluctuations [4]. Anisotropy observed in resistivity [5] also points at stripe formation. Stripe order appears to have an impact on phonon mediated heat transport [6]. Measurements performed by means of NMR and NQR techniques demonstrate the emergence of slow spin fluctuations whose appearance is correlated with pinning of charge-modulations [7]. The distribution of nearest neighbor bond lengths deduced from neutron powder diffraction data [8, 9] and measured by means of extended x-ray-absorption fine structure spectroscopy [10] agrees with expectations based on a scenario of lattice response to local charge-stripe order. An indication of stripe order may be also found by analyzing the shape of ARPES spectra and their evolution with doping. For example, it is natural to expect the Fermi surface to be flat in the stripe phase in the anti-nodal region, near the vectors  $(\pm\pi, 0)$  and  $(0, \pm\pi)$  [4]. In addition, quasi-one-dimensionality of the system should bring about the depletion of spectral weight in the nodal regions, near the Brillouin zone diagonals. Much research has been done to check if these hypotheses are true [4, 11, 12, 13, 14, 15]. It seems that some general structure of spectra may be definitely attributed to an underlying quasi-one dimensional electronic structure [16, 17, 18, 19, 20, 21, 22, 23, 24, 25, 26].

In this paper we will concentrate on doped  $La_{2-x}Sr_xCuO_4$  (LSCO) compounds, slightly above the doping level 1/8 at which, it is believed, a tendency towards nanoscale phase separation seems to be evident in the the ARPES results [12, 15, 27]. In

ARPES intensity maps obtained by integrating over 30 meV at the Fermi energy the spectra from 15% doped  $La_{2-x-y}Nd_ySr_xCuO_4$  (Nd-LSCO) [13], patches with high intensity may be seen in anti-nodal regions. Appreciable spectral weight is also detected at the Fermi energy in nodal regions. A similar pattern of the spectral density at the Fermi energy was predicted by a phenomenological theory of disordered charge stripes and anti-phase spin domains [28]. Unfortunately, this theory does not discuss the origin of renormalized hopping terms in the effective one-body Hamiltonian and does not explain the relation of this renormalization with the underlying magnetic structure. The evolution of the spectral weight as a function of doping has been analyzed for the stripe phase by means of the cluster perturbation technique (CPT) in the framework of the microscopic  $t$ - $J$  and Hubbard models [25]. This theory captures quite well the general trend of this development. Nevertheless, it seems that the spectral weight maps derived within this approach for the doping level at and above 12.5% do not show continuous well developed high-intensity straight patches bridging anti-nodal regions. Such structures are experimentally seen in nodal regions [13]. In addition, that theory does not provide us with much information about the magnetic structure of stripes. The remarks made above seem to suggest that some understanding of the relation between the single particle spectral weight of Nd-LSCO at the filling level about 1/8 and the formation of the stripe phase is missing. A phase which we may expect to emerge in a natural way in weakly doped AFs is a bond-ordered state [29]. Recently, an exact diagonalization of the  $t$ - $J$  model ( $t$ -JM) at a finite cluster has been performed to study stripe formation. It has been shown that the cluster geometry change, from the standard tilted square form of the 20 sites cluster to the rectangular one,  $5 \times 4$  cluster induces the formation of a ground state with pronounced stripe-like charge inhomogeneities [30]. The distribution of peaks in the single-particle spectral weight, which has been calculated by

means of the same method [31], resembles experimental ARPES spectra from  $La_{1.28}Nd_{0.6}Sr_{0.12}CuO_4$  [12]. In particular, the theory captures quite well the strong dispersion along the  $(0, 0)$  -  $(\pi, 0)$  line. The spreading of the quasiparticle-peaks in the single-particle spectrum obtained by means of the exact diagonalization is in good agreement with results of an additional calculation performed by means of a different method which is the bond operator theory for the spin-Peierls phase. Unfortunately, neither the numerical approach nor the analytical method reproduce the flattening of the experimental band near the point  $(\pi, 0)$  and both of them fail to explain the emergence of the spectral weight at the nodal region, in the form of a straight patch which is observed at the Fermi energy in the experiments. Another analysis of the spectral weight in doped AFs, based on the exact diagonalization of a small cluster concerns the  $tJM$  with inhomogeneous terms locally breaking the translational invariance and the spin-rotational SU(2) symmetry [22]. The pattern of the spectral weight at the Fermi energy obtained by means of this method resembles ARPES spectra from Nd-LSCO at the doping level 12% and does not show enhanced intensity at nodal regions. This enhancement observed in experiments is the manifestation of remnant two-dimensionality (2D) in the stripe system. Thus, also this theory seems not account for the shape of ARPES spectra from Nd-LSCO or LSCO at the doping level slightly higher than 1/8.

Results of inelastic neutron scattering (INS) experiments indicate that pronounced AF correlations exist in the stripe phase [2]. On the other hand, the relevance of bond-order has been recently demonstrated by means of the same experimental method [32]. In a recent work [33] we have suggested that the coexistence of bond-order with long range AF order may take place in the stripe phase. The scenario of nanoscale phase separation is realized by means of this coexistence. We have shown in the framework of this concept that above the doping level 1/8, when the distance between stripe axes is 4 lattice spacing a bond-centered stripe with spin-Peierls order on these bonds is more stable than a site-centered stripe. In addition it is also known about the site-centered stripe that it is more stable than a homogeneous system of holes created in the homogeneous AF [19, 34]. The mechanism of coexistence between AF order and spin-Peierls order in the stripe phase is based on lowering the kinetic energy of holes moving without confinement in hole-rich stripes which are formed in the form of two-leg ladder-like domain walls (DWs) between AF hole-poor domains in which the exchange energy decreases [33].

In the next section, in the framework of a scenario for nanoscale phase separation and coexistence of AF long range order with bond-order, we will derive an effective tight-binding Hamiltonian describing a quasiparticle propagating in such a spin background. Next we will calculate the part of the spectral function which is accessible to measurements in photoemission experiments. Finally we will discuss results of the calculation. They seem to

show characteristic features that may be seen in ARPES spectra of Nd-LSCO slightly above the doping level 1/8.

## II. BAND STRUCTURE OF A STRIPE SYSTEM WITH COEXISTING BOND AND AF ORDERS

The  $tJM$  in the framework of which we perform the calculation is

$$H = - \sum_{i,j} t_{ij} c_{i,\sigma}^\dagger c_{j,\sigma} + J \sum_{\langle i,j \rangle} (\mathbf{S}_i \mathbf{S}_j - \frac{n_i n_j}{4}). \quad (1)$$

The states in which any site is doubly occupied have been excluded by definition from the Hilbert space in which that model acts.  $\langle i, j \rangle$  represents pairs of nearest neighbor (NN) sites.  $\vec{S}_i$  and  $n_i$  denote the operators of electron spin and density at site  $i$  respectively.  $t$  represents the hopping matrix element  $t_{i,j}$  between NN sites in the square lattice on which the  $tJM$  is defined,  $t'$  - the hopping matrix element  $t_{i,j}$  between second NN sites, and  $t''$  - the hopping matrix element between third NN sites. The rest of  $t_{i,j}$  is zero. We concentrate on the doping level about 1/8 at which the distance between axes of nearest stripes is 4 lattice spacings and AF correlations seem to be of long range [2]. Our previous analysis has provided convincing arguments that in such a case the stripe takes the form of a two-leg ladder-like DW which separates hole-poor AF domains [33]. The phase of sublattice magnetization in domains changes by  $\pi$  across a DW. Each DW is in the spin-Peierls state with singlets formed on legs. The underlying spin structure of the stripe system at the doping level about 1/8 has been presented in Fig.1. A natural question arises, what is mechanism which gives rise to long range AF correlations, if AF domains are separated by DWs which consist of singlets? The structure depicted in Fig.1 emerges in the presence of holes only. That presence is induced by doping. The creation of a hole gives rise to appearance of an uncompensated spin in the DW. This spin may be parallel or antiparallel to a nearest spin in the neighbor domain. The weight of states in which these spins are antiparallel, Fig.2(a), (b), is higher, because such a configuration is preferred by AF coupling between NN sites. States depicted by Fig.2(a) and (b) are coupled by the hopping term in the Hamiltonian. Since their weight is higher than the weight of states in which an uncompensated spin in the DW and the nearest spin in the domain are parallel, the hopping term which transforms the state depicted by Fig.2 (a) into the state depicted by Fig.2(b), mediates effective ferromagnetic (FM) coupling between sites  $i$  and  $j$ . Some quantum fluctuations will be present in the underlying spin background of the stripe system. They may take the form of triplet excitations on bonds in DWs and multimagnon excitations in domains. Fig.4 in the previous work [33] contains some examples of quantum fluctuations in the spin background. They contribute a lot to the energy of the system. On the other

hand, it seems that quantum fluctuations merely renormalize the shape of quasiparticle dispersion for a given spin background and do not change the picture qualitatively. This has been demonstrated in the case of a hole propagating in the AF spin background [35], as well as in the case of bond ordered two-leg ladders [36, 37] and bond-ordered 2D systems [31]. When it is necessary we will take into account the influence of quantum fluctuations on the distribution of spectral weight. A scenario which underlies the calculation which we are going to outline next, is based on the assumption that hole motion inside ladder-like DWs is governed by the exchange of positions between a hole-fermion pair on a bond and a singlet on a nearby bond [36]. This exchange is mediated by the hopping terms in the initial Hamiltonian (1). We also assume that a hole propagates in the AF spin background as a spin polaron [38]. In the calculation we take into account a simplest form of coupling which moves a hole between a bond ordered DW and an AF domain. This form of coupling originates in the hopping term of the initial Hamiltonian. Before we proceed to construct an effective Hamiltonian which describes the motion of a quasiparticle in the underlying spin background, we will present some formulas which will be useful for that purpose. A singlet on two sites “ $L$ ” and “ $U$ ”, is created in the vacuum by the operator

$$s_{LU}^\dagger = \frac{i}{\sqrt{2}} [\sigma^0 \sigma^y]_{\alpha\beta} c_{L\alpha}^\dagger c_{U\beta}^\dagger. \quad (2)$$

$\sigma^0$  is the two-dimensional identity matrix and  $\sigma^a$ ,  $a = x, y, z$ , are Pauli matrices. The summation over repeating Greek indices is assumed. Three operators which are components of the vector  $\mathbf{t}_{LU}^\dagger$  create three triplet states on sites  $L$  and  $U$ ,

$$\mathbf{t}_{LU}^\dagger = \frac{i}{\sqrt{2}} [\sigma \sigma^y]_{\alpha\beta} c_{L\alpha}^\dagger c_{U\beta}^\dagger. \quad (3)$$

A formula which we will often use later is

$$-c_{U'\sigma}^\dagger c_{U\sigma} (s_{LU}^\dagger c_{L'\gamma}^\dagger) |0\rangle = (\frac{1}{2} s_{L'U'}^\dagger c_{L\gamma}^\dagger + \frac{1}{2} \mathbf{t}_{L'U'}^\dagger \boldsymbol{\sigma}_{\alpha\gamma} c_{L\alpha}^\dagger) |0\rangle. \quad (4)$$

The left side of (4) together with the right-side term which contains a singlet at the pair of sites  $L'$  and  $U'$  represent the exchange of a singlet and a hole-fermion pair between two bonds, which is mediated by the hopping term in the initial Hamiltonian. As we have already stated before, we will neglect the creation of triplets on bonds, however this process also takes place during hole hopping. The creation of a triplet is represented by the second term at the right side of (4). We also need formulas which represent the hopping of a hole from a single site  $i$  which belongs to an AF domain to a site which

belongs to a bond occupied by a singlet and vice versa

$$-c_{i\sigma}^\dagger c_{U\sigma} (s_{LU}^\dagger) |\Omega\rangle = -\frac{i}{\sqrt{2}} \sigma_{\alpha\beta}^y c_{L\alpha}^\dagger c_{i\beta}^\dagger |0\rangle, \quad (5)$$

$$-c_{U\sigma}^\dagger c_{i\sigma} (c_{L\alpha}^\dagger c_{i\beta}^\dagger) |0\rangle = (-\frac{i}{\sqrt{2}} \sigma_{\alpha\beta}^y s_{LU}^\dagger + \frac{i}{\sqrt{2}} [\sigma^y \boldsymbol{\sigma}]_{\alpha\beta} \mathbf{t}_{LU}^\dagger) |0\rangle. \quad (6)$$

When we start to analyze contributions from quantum fluctuations in the ground state of the system to the spectral function we will need followings formulas

$$\mathbf{S}_L \mathbf{S}_i (s_{LU}^\dagger c_{i\beta}^\dagger) |\phi\rangle = \frac{1}{2} \boldsymbol{\sigma}_{\alpha\beta} (\mathbf{t}_{LU}^\dagger c_{i\alpha}^\dagger) |0\rangle, \quad (7)$$

$$\mathbf{S}_U \mathbf{S}_i (s_{LU}^\dagger c_{i\beta}^\dagger) |\phi\rangle = -\frac{1}{2} \boldsymbol{\sigma}_{\alpha\beta} (\mathbf{t}_{LU}^\dagger c_{i\alpha}^\dagger) |0\rangle. \quad (8)$$

We begin the derivation of the effective Hamiltonian describing hole propagation in the spin background depicted by Fig.1 with outlining the mechanism of hole propagation inside an AF domain. A hole created and moving in the Néel background shifts spins between different sublattices and creates defects in the AF structure, Fig.3 (a)-(c). Such a process gives rise to an increase of the Ising energy. This rise is roughly speaking proportional to the length of a path along which the hole has traveled, which means that a tendency towards hole confinement appears [39]. In order to take into account such a tendency we will analyze hole motion in the framework of a basis which consists of states representing holes confined in the AF background by linear defects (strings) left behind by moving holes on their way. We call these states spin polarons. A wave function representing a confined spin polaron at a site  $i$  in an AF domain is a combination of states which are created from the state  $c_{i,\uparrow(\downarrow)}|N\rangle$  by the NN hopping term when a hole created at the site  $i$  starts to move,

$$|\Psi_i\rangle = \sum_{\mathcal{P}_i} \alpha_{l(\mathcal{P}_i)} |\mathcal{P}_i\rangle, \quad (9)$$

$|N\rangle$  is the Néel state in the domain,  $|\mathcal{P}_i\rangle$  denotes a state obtained by hopping along a path  $\mathcal{P}_i$  of a hole created at the site  $i$ .  $\alpha_{l(\mathcal{P}_i)}$  is the amplitude of this state. We have assumed for simplicity that  $\alpha_{l(\mathcal{P}_i)}$  depends solely on the length  $l(\mathcal{P}_i)$  of the path  $\mathcal{P}_i$ . The length of a path or of a string state is defined as the number of hops needed to form a given string state from a state representing a hole created in the AF spin medium. At the first stage of the analysis we take into account only the hopping between NN sites because  $t \gg J, t', t''$ . Processes related to hopping between further neighbors and processes related to swapping antiparallel spins by the transversal term in the exchange interaction will be considered later as a perturbation. A hole moving inside a domain may make its first step in  $(z-1)$  directions.  $z=4$  is the coordination number of the square lattice. There are in principle  $(z-2)$  direction choices of each next hop, if the

hole moves without retracing inside the domain. On the square lattice there are  $z$  choices for the direction of the first step and  $(z - 1)$  for the direction of further hops during the non-retractable motion. These number gets reduced by one for the domain formed by two chains of sites. Thus if we neglect some details, as for example path crossing, we may write,

$$\langle \Psi_i | \Psi_i \rangle = \alpha_0^2 + (z - 1) \sum_{\mu=1} (z - 2)^{\mu-1} \alpha_\mu^2. \quad (10)$$

Each prefactor in (10) at the square  $\alpha_\mu^2$  represents the number of different paths with the length  $\mu$ . We calculate the energy of the spin polaron state  $|\Psi_i\rangle$ ,  $\varepsilon_1$ , which is given by the expectation value of a trial Hamiltonian  $H_0$ ,  $\langle \Psi_i | H_0 | \Psi_i \rangle$ , with the assumption, that the motion of a hole which has started from the site  $i$ , is restricted to the interior of the domain, and that the contribution from the interaction term is restricted to the Ising part  $\sum_{\langle i,j \rangle} (S_i^z S_j^z - \frac{n_i n_j}{4})$ ,

$$\begin{aligned} \langle \Psi_i | H_0 | \Psi_i \rangle &= [3\alpha_0^2 + (z - 1) \sum_{\mu=1} (z - \mu)^{\mu-1} (4 + \mu) \alpha_\mu^2] \frac{J}{2} \\ &+ 2(z - 1) \sum_{\mu=0} (z - 2)^\mu \alpha_\mu \alpha_{\mu+1} t. \end{aligned} \quad (11)$$

The first term in (11) basically counts the number of “broken bonds”, that are not occupied by a pair of antiparallel spins, in which case the Ising contribution to the energy of that bond is higher by  $J/2$  than in the case if it were occupied by a pair of antiparallel spins. The second term in (11) is the contribution from the hopping operator to the spin polaron energy. The prefactors appearing in this term represent the number of paths with a given length multiplied by the number of directions in which these paths may be extended. The appearance of the factor 2 is related to the fact that the hopping which couples paths of length  $\mu$  and  $\mu + 1$  may take place forth and back. The values of these paths  $\alpha_\mu$  can be found by minimizing  $\langle \Psi_i | H | \Psi_i \rangle$  under the constraint  $\langle \Psi_i | H | \Psi_i \rangle = 1$ . After we have constructed spin polarons which are formed in AF domains we are able to present the full basis of single-particle states. The underlying spin background which has been presented in Fig.1 plays the role of the vacuum  $|\Omega\rangle$  for hole-like quasiparticles which propagate in this background.  $|\Omega\rangle$  has been obtained by acting on the absolute vacuum  $|0\rangle$ , in which no particles are present, with a product of operators like  $s_{LU}^\dagger$  creating singlets on bonds connecting sites  $L$  and  $U$  and operators  $c_{i\sigma}^\dagger$  creating spins in domains according to the pattern shown in Fig.1. New fermionic positively charged operators  $h_{i\sigma}^\dagger$  create single particle hole-like states from the vacuum for holes  $|\Omega\rangle$ . The action of the operator  $h_{L\sigma}^\dagger (h_{U\sigma}^\dagger)$  on  $|\Omega\rangle$ , where the site  $L(U)$  belongs to a ladder-like DW, exchanges the operator  $s_{LU}^\dagger$  in the product defining  $|\Omega\rangle$  by the operator  $c_{U\sigma}^\dagger (c_{L\sigma}^\dagger)$ , which means that instead of a singlet on the bond connecting

sites  $L$  and  $U$  there is a hole on the site  $L(U)$  and spin  $\sigma$  on the site  $U(L)$ . The action of the operator  $h_{i\sigma}^\dagger$  on a site  $i$  which belongs to an AF domain, creates a spin polaron  $|\Psi_i\rangle$  in that domain. The spin polaron is a combination of some states, the amplitudes of which are given by prefactors  $\alpha_\mu$ . These states include  $c_{i\bar{\sigma}} |\Omega\rangle$  and states obtained by applying consecutively the NN inside-domain hopping term to the state  $c_{i\bar{\sigma}} |\Omega\rangle$ . During this process, the hole hops without retraces and  $\mu$  is  $l(\mathcal{P}_i)$ , the length of the path  $\mathcal{P}_i$ , along which the hole has traveled to form a given component state of  $|\Psi_i\rangle$ . A label which we will use to mark the fermionic operator creating either a bond hole or a hole-like spin polaron at a give site is  $(m,n)_{i,j}$ .  $m$  refers to the column number of the unitary cell to which belongs the site where the hole-like particle has been created,  $n$  refers to the row number of the unitary cell, and  $i$  (column),  $j$  (row) are indices representing the position of that site inside the unitary cell.  $i$  and  $j$  run from 0 to 7 and from 0 to 1, respectively. Now we start to explain with some details the origin of contributions to the effective Hamiltonian for a single quasiparticle propagating in the spin background depicted by Fig.1 which is an exemplification of coexistence between AF and bond orders. We concentrate on the case of a spin-up quasiparticle. Within the approximation which we use, operators  $h_{i\uparrow}^\dagger$  create in the vacuum  $|\Omega\rangle$  eigenstates of the unperturbed Hamiltonian  $H_0$ ,

$$H_0 = \sum_{\langle i,j \rangle} S_i S_j - t \sum_{\langle i',j' \rangle} c_{i\sigma}^\dagger c_{j\sigma} + J \sum_{\langle i',j' \rangle} (S_i^z S_j^z - \frac{n_i n_j}{4}) \quad (12)$$

where  $\langle i,j \rangle$  are pairs of sites on which singlets depicted in Fig.1 have been formed and  $\langle i',j' \rangle$  are pairs of NN sites belonging to AF domains. Action of  $H_0$  is restricted to the space containing states in which none of the sites is doubly occupied. This Hamiltonian contains the Ising part of the exchange energy of links inside domains. It also drives hole hopping between NN sites inside each domain. Since all matrix elements which may give rise to deconfinement of a hole, have been by definition removed from  $H_0$ , polaron states  $|\Psi_i\rangle$  are its eigenstates. Processes which bring about deconfinement of holes will be treated at the latter stage of the calculation as a perturbation. The exchange energy and the hopping between sites belonging to bonds occupied by singlets in Fig.1 are the only contribution to the Hamiltonian  $H_0$  from DWs. Terms in the Hamiltonian of the  $tJM$  which couple a site belonging to a ladder-like DW with a site belonging to a domain do not contribute to  $H_0$ . It is clear that the vacuum state  $|\Omega\rangle$  and the single particle states  $h_{i\sigma}^\dagger |\Omega\rangle$  are eigenstates of  $H_0$ . Within the first order approximation the on-site energy of a quasiparticle with spin up created at the site  $(m,n)_{0,1}$  which belongs to a DW is  $2J$ . From now on, the reference value of the energy is the energy of the vacuum state  $|\Omega\rangle$ . The contribution from a destroyed singlet to the on-site energy of a hole-like quasiparticle created at the site  $(m,n)_{0,1}$  is  $(3/4)J$ . A hole-like quasipar-

ticle occupying the site  $(^{m,n}_{0,1})$  with spin up is by definition the same as a single fermion with spin up which occupies the site  $(^{m,n}_{0,0})$  belonging to the bond  $(^{m,n}_{0,0})-(^{m,n}_{0,1})$ . Since spins on the sites  $(^{m,n}_{0,0})$  and  $(^{m-1,n}_{7,0})$  are in this case parallel, the lowest order contribution to the exchange energy of the bond between these two sites additionally increases by  $J/4$  compared to the contribution from this bond in the vacuum state  $|\Omega\rangle$ . In the presence of a hole, the contribution from the potential term  $-\sum_{\langle i,j \rangle} n_i n_j / 4$  in the initial Hamiltonian of the  $tJM$  is higher by  $J$ . By adding all partial contribution we get the value  $2J$  of the total on-site energy of the spin-up quasiparticle at the site  $(^{m,n}_{0,1})$ . The same on-site energy have spin up quasiparticles created in DWs at all sites which are NN of sites in domains occupied by spins pointing down. Finally we deduce that in the effective single-particle Hamiltonian appears a term

$$\begin{aligned} \delta_1 H_{eff} = & 2J \sum_{m,n} [h_{(^{m,n}_{0,1})\uparrow}^\dagger h_{(^{m,n}_{0,1})\uparrow} + h_{(^{m,n}_{1,1})\uparrow}^\dagger h_{(^{m,n}_{1,1})\uparrow} \\ & + h_{(^{m,n}_{4,0})\uparrow}^\dagger h_{(^{m,n}_{4,0})\uparrow} + h_{(^{m,n}_{5,0})\uparrow}^\dagger h_{(^{m,n}_{5,0})\uparrow}]. \end{aligned} \quad (13)$$

The fermionic operators  $h_{(^{m,n}_{i,j})}^\dagger$  and  $h_{(^{m,n}_{i,j})}$  transform the underlying vacuum  $|\Omega\rangle$  into the single particle state described above and the single particle state into  $|\Omega\rangle$ , respectively. The notation for indices which we use seems not to be very short, but such a form of it is basically unavoidable because the elementary cell of the underlying spin background, Fig.1, is rather big. That notation also helps to trace easily at the map which is Fig.1, the results of hopping events mediated by the Hamiltonian  $H_{eff}$ . An analogous term will appear in the Hamiltonian representing a propagating spin-down quasiparticle, but with a different set of indices labelling sites in the elementary cell. The creation of the spin down quasiparticle at these sites,  $(0,0), (1,0), (4,1), (5,1)$  induces the formation at the ladder leg of an uncompensated spin, the direction of which is parallel to the direction of the nearest spin in the domain. For the sake of simplicity we will concentrate in this paper on the propagation of the spin-up quasiparticle. Such a simplification is possible because despite the breakdown of the time reversal symmetry by the underlying spin structure, the energy of the spin-up and the spin-down quasiparticles is degenerate. Later we will user this observation in the calculation. The on-site energy of the hole-like quasiparticle is lower for a group of sites by  $J/2$  then for sites to which the contribution (13) refers because spin of the bond-fermion which appears after a hole has been created at a bond initially occupied by a singlet may be antiparallel to the nearest spin in one of domains,

$$\begin{aligned} \delta_2 H_{eff} = & \frac{3}{2} J \sum_{m,n} [h_{(^{m,n}_{0,0})\uparrow}^\dagger h_{(^{m,n}_{0,0})\uparrow} + h_{(^{m,n}_{1,0})\uparrow}^\dagger h_{(^{m,n}_{1,0})\uparrow} \\ & + h_{(^{m,n}_{4,1})\uparrow}^\dagger h_{(^{m,n}_{4,1})\uparrow} + h_{(^{m,n}_{5,1})\uparrow}^\dagger h_{(^{m,n}_{5,1})\uparrow}]. \end{aligned} \quad (14)$$

Let us concentrate now on the on-site energy of quasiparticles created at sites belonging to domains. A spin-up hole-like spin polaron can by definition be created exclusively at sites which have been initially occupied by a spin-down fermion. An obvious contribution to the on-site energy of a hole-like quasiparticle energy in domains is  $\varepsilon_1$ , the minimum value of the matrix element (11) obtained under the constraint  $\langle \Psi_i | \Psi_i \rangle = 1$ . During the construction of spin polarons we have considered only hopping between NN sites, which is governed by the hopping with the highest integral  $t$ . We have also neglected some “high order” processes related to path crossing or to the action of the XY term in the Heisenberg model. In the analysis which we start now, we will discuss in the framework of the first order perturbation theory the contribution of some neglected processes to the effective Hamiltonian  $H_{eff}$ . States depicted by Figs.4(b) and (c) are string states of length 1 and are components of the spin-polaron wave-function  $|\Psi_i\rangle$  at the site  $i$ . A single vertical or horizontal hop of the hole created in the AF background at the site  $i$  gives rise to the states depicted by Figs.4(b) and (c) respectively. The hopping term to next nearest neighbors (NNN) which we treat as a perturbation couples states represented by Figs.4(b) and (c), which brings about a contribution to the matrix element  $\langle \Psi_i | H_1 | \Psi_i \rangle$ , where  $H_1 = H - H_0$ . This contribution is

$$\gamma_1 = 4t' \alpha_1^2. \quad (15)$$

We recognize in (15) a product of amplitudes with which string states of length 1 appear in the definition (9) of the spin polaron state. The factor 4 which appears in (15) is related to the fact that hopping which couples states (b) and (c) may occur in both directions and that analogous coupling takes place between the state depicted by Fig.4(c) and the state depicted by Fig.4(d). The state depicted by Fig.4(d) has been obtained by a single downward hop of a hole created in the AF domain at the site  $i$ . The contribution

$$\gamma_2 = 2t'' \alpha_1^2 \quad (16)$$

to  $\langle \Psi_i | H_1 | \Psi_i \rangle$  originates in a similar way with coupling between states depicted in Fig.4(c) and (d) by the hopping term to third nearest neighbor (TNN) sites. The coupling between longer string states which are components of the same spin-polaron wave-function may also contribute to the renormalization of the spin-polaron on-site energy. To be more specific, the coupling between states as depicted by Figs.4(e) and (f) and between their reflections in the horizontal line running through the site  $i$  gives rise to the correction

$$\gamma_3 = 2t'[2\alpha_2^2 + (z-1) \sum_{\mu=3} (z-2)^{\mu-3} \alpha_\mu^2] \quad (17)$$

to  $\langle \Psi_i | H_1 | \Psi_i \rangle$ , while the coupling between the state depicted by Fig.4(g) and its reflection in the horizontal line running through the site  $i$  together with some similar

process in which longer strings are involved brings about the correction

$$\gamma_4 = 2t''[\alpha_2^2 + (z-1) \sum_{\mu=3} (z-2)^{\mu-3} \alpha_\mu^2]. \quad (18)$$

The states represented by Figs.4(e), (f) and (g) have been obtained by means of three different sequences of hole moves. The hole has been created at the site  $i$  and these sequences are upwards-upwards, upwards-left and left-upwards respectively. Longer strings pinned to the site  $i$  may be coupled in a very similar way, which also gives rise to a change of the on-site energy. This change has actually already been incorporated into parameters  $\gamma_3$  and  $\gamma_4$ . Finally, by collecting all terms we may infer that in the effective Hamiltonian  $H_{eff}$  appears the following term referring to the on-site energy of spin-polarons

$$\begin{aligned} \delta_3 H_{eff} = & (\varepsilon_1 + \gamma_1 + \gamma_2 + \gamma_3 + \gamma_4 + J/4) \\ & \times \sum_{m,n} [h_{(2,1)}^\dagger h_{(2,1)}^{(m,n)\uparrow} + h_{(3,0)}^\dagger h_{(3,0)}^{(m,n)\uparrow} \\ & + h_{(6,0)}^\dagger h_{(6,0)}^{(m,n)\uparrow} + h_{(7,1)}^\dagger h_{(7,1)}^{(m,n)\uparrow}]. \end{aligned} \quad (19)$$

The additional term  $J/4$  in the prefactor is related to the fact that the contribution from the contact interaction  $-Jn_i n_j/4$  between a site  $i$  in a domain and a site  $j$  in a DW is higher by  $J/4$ , when a hole is created in the domain at the site  $i$ . This interaction was neglected, when we were calculating the eigenenergy  $\varepsilon_1$  of the spin polaron and needs to be taken into account now. (19) is the last on-site term in the effective Hamiltonian.

The NN hopping integral for the quasiparticle, the propagation of which we describe in this paper is the same as the bare hopping integral provided that the sites between which the quasiparticle moves belong to the same initially ordered bond inside a DW [33]. Thus, the term which describes the quasiparticle hopping between NN sites, on which singlets have been formed in the underlying spin background, takes the following form

$$\begin{aligned} \delta_4 H_{eff} = & -t \sum_{m,n} \{ [h_{(0,1)}^\dagger h_{(0,0)}^{(m,n)\uparrow} + h_{(1,1)}^\dagger h_{(1,0)}^{(m,n)\uparrow} \\ & + h_{(4,1)}^\dagger h_{(4,0)}^{(m,n)\uparrow} + h_{(5,1)}^\dagger h_{(5,0)}^{(m,n)\uparrow}] + H.c.\}. \end{aligned} \quad (20)$$

The NN hopping integral for a pair of sites, which belong to different singlets in the underlying insulating state is  $t/2$  instead of  $-t$ . This change of sign and this reduction of size may be deduced from the form of the first term on the right side of Eq.(4). Therefore, we may write the following expression for the contribution to the effective Hamiltonian describing quasiparticle hopping between NN sites belonging to different bonds on which singlets has been

formed in the underlying spin background

$$\begin{aligned} \delta_5 H_{eff} = & \frac{t}{2} \sum_{m,n} \{ [h_{(1,0)}^\dagger h_{(0,0)}^{(m,n)\uparrow} + h_{(0,1)}^\dagger h_{(0,0)}^{(m,n)\uparrow} \\ & + h_{(1,1)}^\dagger h_{(0,1)}^{(m,n)\uparrow} + h_{(1,1)}^\dagger h_{(1,0)}^{(m,n)\uparrow} \\ & + h_{(5,0)}^\dagger h_{(4,0)}^{(m,n)\uparrow} + h_{(4,1)}^\dagger h_{(4,0)}^{(m,n)\uparrow} \\ & + h_{(5,1)}^\dagger h_{(4,1)}^{(m,n)\uparrow} + h_{(5,1)}^\dagger h_{(5,0)}^{(m,n)\uparrow}] + H.c.\}. \end{aligned} \quad (21)$$

The value of the NN hopping integral, between a site which belongs to a domain and a site which belongs a DW, can be inferred from the first part of the right side in Eq.(6),

$$\begin{aligned} \delta_6 H_{eff} = & -\frac{t}{\sqrt{2}} \alpha_0 \sum_{m,n} \{ [h_{(7,1)}^\dagger h_{(0,1)}^{(m,n)\uparrow} \\ & + h_{(2,1)}^\dagger h_{(1,1)}^{(m,n)\uparrow} + h_{(3,0)}^\dagger h_{(4,0)}^{(m,n)\uparrow} \\ & + h_{(6,0)}^\dagger h_{(5,0)}^{(m,n)\uparrow}] + H.c.\}. \end{aligned} \quad (22)$$

Since the time reversal symmetry and the translational symmetry are broken inside AF domains, the propagating quasiparticle can not move between different sublattices and any term related to NN hopping inside domains is not generated in the effective Hamiltonian  $H_{eff}$ . NNN quasiparticle hopping inside DWs and hopping between sites which belong to a DW and a domain is a first order process that is mediated by the NNN hopping term in the bare Hamiltonian. The explicit forms of related contributions to  $H_{eff}$  may be deduced from formulas (4), (5) and (6),

$$\begin{aligned} \delta_7 H_{eff} = & \frac{t'}{2} \sum_{m,n} \{ [h_{(1,1)}^\dagger h_{(0,0)}^{(m,n)\uparrow} \\ & + h_{(1,1)}^\dagger h_{(0,0)}^{(m,n)\uparrow} + h_{(1,0)}^\dagger h_{(0,1)}^{(m,n)\uparrow} \\ & + h_{(0,1)}^\dagger h_{(1,0)}^{(m,n)\uparrow} + h_{(5,1)}^\dagger h_{(4,0)}^{(m,n)\uparrow} \\ & + h_{(5,1)}^\dagger h_{(4,0)}^{(m,n)\uparrow} + h_{(5,0)}^\dagger h_{(4,1)}^{(m,n)\uparrow} \\ & + h_{(4,1)}^\dagger h_{(5,0)}^{(m,n)\uparrow}] + H.c.\}, \end{aligned} \quad (23)$$

$$\begin{aligned} \delta_8 H_{eff} = & -\frac{t'}{\sqrt{2}} \alpha_0 \sum_{m,n} \{ [h_{(7,1)}^\dagger h_{(0,0)}^{(m,n)\uparrow} \\ & + h_{(7,1)}^\dagger h_{(0,0)}^{(m,n)\uparrow} + h_{(2,1)}^\dagger h_{(0,0)}^{(m,n)\uparrow} \\ & + h_{(2,1)}^\dagger h_{(0,0)}^{(m,n)\uparrow} + h_{(3,0)}^\dagger h_{(4,1)}^{(m,n)\uparrow} \\ & + h_{(3,0)}^\dagger h_{(4,1)}^{(m,n)\uparrow} + h_{(6,0)}^\dagger h_{(5,1)}^{(m,n)\uparrow} \\ & + h_{(6,0)}^\dagger h_{(5,1)}^{(m,n)\uparrow}] + H.c.\}. \end{aligned} \quad (24)$$

The task of finding the formula for the term describing NNN hopping inside AF domains is little bit more

tedious. For example the coupling by the XY term in the Heisenberg model between string states depicted by Fig.4(f) and (h) gives rise to hopping terms in  $H_{eff}$  which shift a spin polaron from the site  $i$  to the site  $j$  and vice versa. We analyze now the XY term, because it has been neglected during the first stage of the analysis, when quasi-confined spin polaron states have been constructed. Since the string state depicted by Fig.4(f) is a component of the wave function  $|\Psi_i\rangle$  for the spin polaron created at the site  $i$  and the string state depicted by Fig.4(h) is evidently a component of the wave function for the spin polaron created at the site  $j$ , the coupling between these components gives rise to the coupling between spin polaron states  $|\Psi_i\rangle$  and  $|\Psi_j\rangle$ . This brings about a contribution to the matrix element  $\langle\Psi_j|H|\Psi_i\rangle$  and to the hopping term in the effective Hamiltonian  $H_{eff}$ . It is probably useful to remind now that  $H_{eff}$  is an approximation to the initial Hamiltonian  $H$  in (1). This approximation is expressed in terms of the operators creating and annihilating spin polarons. Also the coupling between the states depicted by Fig.4(g) and (h) contributes to the hopping term between the sites  $i$  and  $j$  in the effective Hamiltonian  $H_{eff}$ . This coupling is mediated by the XY term. We have already discussed the action of the XY term which by removing two defects in the AF structure transforms string states of length 2, tails of which are pinned to the site  $i$ , into the state representing a hole created at the site  $j$  in the AF ordered domain. By a string tail we mean its end opposite the end at which sits a hole. The XY term may also transform a state representing a hole created in the domain at the site  $i$  into a string state of length 2 pinned at the tail to the site  $j$ . This additional coupling between components of the spin polaron states at the sites  $i$  and  $j$  doubles the value of the hopping integral between these sites in the effective Hamiltonian. Thus, after a little thought we may deduce that the integral for the NNN hopping inside domains is

$$\tau_1 = 2J \sum_{\mu=2} (z-2)^{\mu-2} \alpha_\mu \alpha_{\mu-2}. \quad (25)$$

The first term in the sum presented above refers to coupling between strings of length 0 and 2. We have just outlined its origin in detail. Other terms appear in the sum (25) because longer strings, which are created when a hole moves further from the site  $j$  in Figs.4(f), (g) and (h), are also coupled by the XY term in the Heisenberg model. The hop left of the hole depicted by Fig.4(g) gives rise to the string state of length three, Fig.4(i), which is pinned to the site  $j$ . Since we neglected the possibility of path crossing when we were constructing the quasiconfined spin-polaron states, some corrections need to be made now. For example we did not consider before, that by applying the NN hopping term to the state depicted by Fig.4(i) we may create the state depicted by Fig.4(j). Since the latter state is a string-like component of the spin-polaron at the site  $j$  obtained by hopping downward and left of a hole created at that site, we deduce that the process described above generates the

NNN hopping term in the effective Hamiltonian with the amplitude

$$\tau_2 = 2t\alpha_3\alpha_2. \quad (26)$$

The factor 2 originates with the fact that the motion of a hole around a plaque in the square lattice may take place clockwise and anti-clockwise. We also recognize  $\alpha_3$  and  $\alpha_2$  as amplitudes of strings, which have the length 3 and 2, respectively. Exactly such strings which are components of the spin-polaron states at the sites  $i$  and  $j$  in Figs.4(i), (j) are coupled by the NN hopping term in the initial Hamiltonian. The NNN term in the initial Hamiltonian generates coupling between states representing “bare” holes created in the AF background of domains. Since these states are also string components with the length 0 of some spin polaron wave functions, coupling between the latter is also generated. An example of such coupled string states are Figs.4(h) and (k). The contribution to the NNN hopping integral in  $H_{eff}$  is

$$\tau_3 = t'\alpha_0^2. \quad (27)$$

The NNN term in the bare Hamiltonian also couples states depicted by Figs.4(f) and (l) which are string-like components with length 2 of spin-polaron states at the sites  $i$  and  $j$ , respectively. The coupling amplitude is

$$\tau_4 = 2t'\alpha_2^2. \quad (28)$$

The appearance of the factor 2 is related to the fact that states which are created when holes move between the sites  $i$  and  $j$  in opposite directions around the plaque, than in the case of the states depicted by Figs.4(f) and (l) are also coupled by the bare NNN hopping. The state in Fig.4(l) has been obtained by hopping left and downward of a hole which has been initially created at the site  $j$ . By collecting all contributions, which we have discussed above, we see that the new term in to  $H_{eff}$  is,

$$\begin{aligned} \delta_9 H_{eff} = & (\tau_1 + \tau_2 + \tau_3 + \tau_4) \\ & \times \sum_{m,n} \{ [h_{(3,0)}^\dagger h_{(2,1)}^{(m,n)} + h_{(2,1)}^\dagger h_{(3,0)}^{(m,n)} \\ & + h_{(7,1)}^\dagger h_{(6,0)}^{(m,n)} + h_{(7,1)}^\dagger h_{(6,0)}^{(m,n)}] + H.c. \}. \end{aligned} \quad (29)$$

By means of a similar analysis, as for the hopping between NNN sites we may find the TNN hopping term in the effective Hamiltonian. For the operator representing the quasiparticle hopping inside DWs we get

$$\begin{aligned} \delta_{10} H_{eff} = & \frac{t''}{2} \sum_{m,n} \{ [h_{(0,0)}^{(m,n+1)} h_{(0,0)}^{(m,n)} \\ & + h_{(0,1)}^{(m,n+1)} h_{(0,1)}^{(m,n)} + h_{(1,0)}^{(m,n+1)} h_{(1,0)}^{(m,n)} \\ & + h_{(1,1)}^{(m,n+1)} h_{(1,1)}^{(m,n)} + h_{(4,0)}^{(m,n+1)} h_{(4,0)}^{(m,n)} \\ & + h_{(4,1)}^{(m,n+1)} h_{(4,1)}^{(m,n)} + h_{(5,0)}^{(m,n+1)} h_{(5,0)}^{(m,n)} \\ & + h_{(5,1)}^{(m,n+1)} h_{(5,1)}^{(m,n)}] + H.c. \}. \end{aligned} \quad (30)$$

The TNN hopping of the quasiparticle between domains and DWs is governed by the following term

$$\begin{aligned} \delta_{11}H_{eff} = & -\frac{t''}{\sqrt{2}}\alpha_0 \sum_{m,n} \{ [h_{(m-1,n)}^\dagger h_{(0,0)}^{\downarrow}] \\ & + h_{(2,1)}^\dagger h_{(0,1)}^{\downarrow} + h_{(3,0)}^\dagger h_{(1,0)}^{\downarrow} \\ & + h_{(7,1)}^\dagger h_{(1,1)}^{\downarrow} + h_{(6,0)}^\dagger h_{(4,0)}^{\downarrow} \\ & + h_{(2,1)}^\dagger h_{(4,1)}^{\downarrow} + h_{(3,0)}^\dagger h_{(5,0)}^{\downarrow} \\ & + h_{(7,1)}^\dagger h_{(5,1)}^{\downarrow}] + H.c.\}. \end{aligned} \quad (31)$$

To TNN hopping term between sites in domains contribute: a) the mechanism which is based on the shortening of strings by the action of the XY term, b) the coupling of strings with length 0 by the TNN hopping term in the initial Hamiltonian and c) the exchange between the head and the tail of a straight string with length 2. The last process is mediated by the TNN hopping term in the initial Hamiltonian (1).

The contributions to the hopping integral in these three cases are

$$\tau_5 = 2J \sum_{\mu=2} (z-2)^{\mu-2} \alpha_\mu \alpha_{\mu-2}, \quad (32)$$

$$\tau_6 = t'' \alpha_0^2, \quad (33)$$

$$\tau_7 = t'' \alpha_2^2. \quad (34)$$

Since the origin of these couplings is the same as for the NNN hopping term in  $H_{eff}$  we do not discuss them in detail. Thus, the TNN hopping operator, which is the last contribution to  $H_{eff}$  discussed by us at the approximation level, that we have assumed, takes the form,

$$\begin{aligned} \delta_{12}H_{eff} = & (\tau_5 + \tau_6 + \tau_7) \sum_{m,n} \{ [h_{(m-1,n+1)}^\dagger h_{(2,1)}^{\downarrow}] \\ & + h_{(m,n+1)}^\dagger h_{(3,0)}^{\downarrow} + h_{(m,n+1)}^\dagger h_{(6,0)}^{\downarrow} \\ & + h_{(m,n+1)}^\dagger h_{(7,1)}^{\downarrow}] + H.c.\}. \end{aligned} \quad (35)$$

Fig.6 depicts the electronic structure which we have obtained by solving the Hamiltonian  $H_{eff}$ . It represents the energy dispersion  $E(\mathbf{p})$  of all bands along the line  $(0,0)$ - $(\pi,0)$ - $(\pi,\pi)$ - $(0,0)$  and the line obtained by performing the rotation by  $\pi/2$  around the point  $(0,0)$ . Such a combination of dispersion curves is justified by conditions in which experiments are performed, because it seems that stripes in some regions of the sample may run vertically, while in other regions they may run horizontally. The reason for this mixing can be, for example, sample twinning. Nondispersing parts of bands are related to some obstacles for hole propagation in the directions perpendicular to stripes. That kind of motion seems to be blocked, which is clear because  $H_{eff}$  by definition can not mediate quasiparticle motion occurring exclusively in the direction perpendicular to stripes. It seems that

the lack of the energy dispersion in some directions accounts for straight patches of the spectral weight which appear in the density maps obtained by means of ARPES measurements [40]. The coordination frame applied to draw these maps is the same as we have used to obtain Fig.6 (momentum-energy), while the second derivative of ARPES spectra plays the role of a density-like parameter which marks regions with the high spectral weight [27]. We shall make a more detailed comparison with ARPES spectra, after we calculate the spectral weight by means of the approach applied by us. That approach is based, as we have already mentioned several times, on a combination of bond and string formalisms.

### III. SINGLE PARTICLE SPECTRAL FUNCTION IN THE STRIPE PHASE WITH COEXISTING BOND AND AF ORDERS

ARPES probes the one-particle spectral function  $A^-(\mathbf{k}, \omega)$ . We neglect in the further analysis of ARPES spectra the influence of temperature. We also assume that the description of the photoelectric effect in terms of Fermi's golden rule is sufficient and finally we omit, in the calculation, electromagnetic dipole matrix elements between the wave function of photoelectron and the wave functions of the electrons in the initial states. Furthermore, we apply the single particle approximation, in the calculation of the spectral function  $A^-(\mathbf{k}, \omega)$ , which is natural, because the Hamiltonian  $H_{eff}$  by definition does not contain the interaction terms. Since electrons are emitted by the photoelectric effect, at  $T = 0$  information is gathered only about the one-electron removal part of the spectral function, which takes the form

$$A^-(\mathbf{k}, \omega) = \sum_m |\langle \Psi_m^{N-1} | c_{\mathbf{k}} | \Psi_i^N \rangle|^2 \delta(\omega + E_m^{N-1} - E_i^N). \quad (36)$$

Due to the formation of the stripe structure the shape of which is determined by the underlying spin background depicted by Fig.1, the 1BZ gets reduced by a factor of 8 in the horizontal direction and by a factor of 2 in the vertical direction. The Hamiltonian  $H_{eff}$  may be written in the diagonal form in terms of operators  $h_{\mathbf{k}, \uparrow, \alpha}^\dagger$ , and their Hermitian conjugates, which are determined by the form of Hamiltonian eigenstates,

$$h_{\mathbf{k}_R, \uparrow, \alpha}^\dagger = \frac{1}{\sqrt{NL}} \sum_{n,l} e^{i\mathbf{k}_R(nd, lw)} \sum_{i,j} F_{\mathbf{k}_R, (i,j), \uparrow, \alpha} h_{(i,j)}^\dagger \quad (37)$$

where  $\mathbf{k}_R$  belongs to the reduced 1BZ,  $\alpha$  labels the band number,  $d = 8$  is the length of the elementary supercell,  $w = 2$  is the width of the elementary supercell and  $Nd \times Lw$  is the system size. Thus, within the single-particle approach, the one-electron removal part of the spectral

function is approximated as

$$\begin{aligned} A^-(\mathbf{k}, \omega) &= \sum_{\alpha} \delta(\omega + \varepsilon_{\mathbf{k}, \alpha}) \\ &\times \left| \sum_{n, l} \sum_{i, j} \sum_{i', j'} F_{\mathbf{k}, \text{modK}_R, (i, j); \uparrow, \alpha}^* e^{i\mathbf{k}(nd, lw)} \right. \\ &\times \left. e^{-i\mathbf{k}(i', j')} \langle \Omega | h_{(i, j)}^{(n, l)} \uparrow c_{(i', j')}^{(0, 0)} \downarrow | \Omega \rangle \right|^2, \end{aligned} \quad (38)$$

where  $\mathbf{k}\text{modK}_R$  denotes the vector  $\mathbf{k}$  reduced to the 1BZ of the superlattice, the elementary cell of which is depicted by Fig.1 and  $\varepsilon_{\mathbf{k}, \alpha}$  is the energy of the  $\alpha$ -th band in Fig.6. In order to evaluate (38) we need to find matrix elements,

$$M_{(i, j)(i', j')} = \langle \Omega | h_{(i, j)}^{(n, l)} \uparrow c_{(i', j')}^{(0, 0)} \downarrow | \Omega \rangle. \quad (39)$$

A scheme showing how to do this in the framework of the spin polaron (string) approach was developed before [41]. For example, the removal of the spin down electron at the site  $(2, 1)$  in the elementary cell of the underlying spin background depicted by Fig.1 gives rise to a state which is component of the wave function for the polaron created at this site. Thus the matrix element (39) for  $(i', j') = (i, j) = (2, 1)$  and  $(n, l) = 0$  is  $\alpha_0$ . In the appendix we list all sites labelled by the pairs of numbers  $(i', j')$ ,  $(n, l)$ ,  $(i, j)$ , for which a nonvanishing matrix element (39) exists. The removal of a spin down electron from a site which belongs to ladder-like DWs in the state depicted by Fig.1 gives rise to the hole-like quasiparticle  $h$  at this site. Since this removal may be mediated by the electron annihilation operator  $c$  in (39), a nonvanishing diagonal matrix element  $M = -1/\sqrt{2}$  is generated. Quantum spin fluctuation which are generated in the underlying spin background schematically depicted by Fig.1 can not be neglected when we evaluate the spectral function. Within the first order perturbation theory the admixture  $\delta|\phi\rangle$  of quantum fluctuations to the groundstate  $|\phi_0\rangle$  of  $H_0$  brought about by the perturbation  $H_1$  is

$$\delta|\phi\rangle = - \sum_n \frac{\langle \psi_n | H_1 | \phi_0 \rangle}{E_n - E_0} |\psi_n\rangle, \quad (40)$$

where  $|\psi_n\rangle$  are excited eigenstates of  $H_0$  with energies  $E_n$  and  $E_0$  is the groundstate energy. The action of the exchange interaction between sites depicted by Fig.5(a),  $L(U)$  belonging to a DW and  $i(j)$  belonging to an AF domain, may transform the singlet on sites  $L$  and  $U$  into a triplet. Within our approach we treat this part of the exchange interaction as the perturbation. The transformed state is an excited eigenstate of  $H_0$  with the energy  $J$  and also a quantum fluctuation that, according to the formula (40), contributes to the underlying vacuum state  $|\Omega\rangle$ , about which we assume that it is an eigenstate of the Hamiltonian (1).  $|\Omega\rangle$  is schematically depicted by Fig.1 in which quantum corrections have not been taken into account even within the framework of the first order perturbation theory. The electron annihilation operator  $c$  that acts on a site belonging to a bond, which has been

excited to the triplet state, transforms it into the state representing the hole-like quasiparticle  $h$  created at that site. This process gives rise an addendum to the matrix element (39). This addendum may be attributed to the existence of quantum corrections to the vacuum state  $|\Omega\rangle$ . For example the value of this addendum is  $-1/(2\sqrt{2})$  for the matrix element (39) labelled by the indices  $(i', j') = (i, j) = (n, l) = (0, 0)$ . The XY part of the exchange interaction which we treat as a perturbation, creates in  $|\Omega\rangle$  an excitation that takes the form of two NN spins turned upside down, Fig.5(b), with respect to the underlying spin structure, Fig.1. According to the recipe (40) this excitation contributes a correction to the underlying vacuum state  $|\Omega\rangle$ . If the annihilation operator  $c$  removes the spin down fermion at the site  $j$  in Fig.5(b), the configuration depicted by Fig.5(c) will be created, which is a string state, a component of the wave function  $|\psi_i\rangle$  for the spin polaron at the site  $i$ . Since this spin polaron state is by definition created by the fermionic operator  $h^\dagger$  a contribution  $-\alpha_1/4$  to some diagonal matrix elements of the form (39) is generated. We discuss now the last category of processes which give rise to new terms in the sum that appears in (38). The electron removal from the site  $k$ , Fig.4(b), gives rise to a string state of length 2, Fig.4(d), which is a component of the wave function for the spin polaron at the site  $i$ . Since the spin-polaron state is created by the operator  $h^\dagger$ , a nonvanishing matrix element is generated. Its value is  $-\alpha_2/4$ , which gets multiplied by a factor of 2, because there are two strings of length two, connecting sites  $i$  and  $k$ . By collecting all contributions to the sum which appears in (38) the one-electron removal part of the spectral function  $A^-(\mathbf{k}, \omega)$  can be evaluated. We will apply in the numerical evaluation some Lorentzian broadening of the Dirac delta function, which is justified because experimental measurements, with which we are going to compare our results, have finite resolution and also some averaging procedure is often applied to present experimental data.

#### IV. NUMERICAL EVALUATION OF THE SPECTRAL WEIGHT, COMPARISON WITH RESULTS OF ARPES EXPERIMENTS AND CONCLUDING REMARKS

It seems that a most complete set of data to compare with our theoretical analysis, provide ARPES measurements of the LSCO and Nd-LSCO systems not for the doping level  $x = 0.125$  but for the doping level  $x = 0.15$  [12, 13, 27, 40]. We will present our results in a way similar to the method of presentation, which was used in experimental papers reporting these measurements. The NN hopping parameter  $t$  defines a unit in which energy is measured. We choose  $J/t = 0.4$ ,  $t'/t = -0.1$ ,  $t''/t = 0.05$ . Similar parameters have been applied in a recent theoretical analysis of ARPES spectra in the 2D  $tJM$ , based on the exact diagonalization of the  $5 \times 4$

cluster and in a separate calculation performed by means of the bond operator formalism applied to the columnar bond order underlying spin structure [31]. This coincidence helps to make comparison between results of the calculation presented in our paper and results of the earlier analysis. The choice of the Hamiltonian parameters is ever to some extent arbitrary. On the other hand a theoretical analysis of ARPES spectra from LSCO systems, based on the tight binding approach indicates that the ratios  $|t'/t|$  and  $|t''/t|$  are lower for these systems than for other members of cuprate family [42]. Parameters suggested by the authors of the analysis based on a tight binding approach [42] are basically the same as parameters applied in our calculation. The position of the Fermi energy in the band structure at the doping level 15% has been determined in our calculation by counting the number of hole-like states. It has been marked as a narrow straight line in Fig.6. Fig.7 depicts the intensity of the one-electron removal spectrum function presented in the coordination frame momentum-energy. Contributions from vertical and horizontal stripes have been summed in order to account for presumed coexistence of these structures in different parts of the sample. In some agreement with the experimental result obtained at the doping level 15% [27] we notice in the calculated spectrum a strongly dispersing band between points  $(0, 0)$  and  $(\pi, 0)/(0, \pi)$  which approaches the Fermi level,  $\omega = 0$ , near the zone boundary, where it joins a flat patch formed by the region of high spectral intensity. After passing the anti-nodal region as a straight narrow strip, the band-like region of high intensity disappears somewhere between  $(\pi, 0)/(0, \pi)$  and  $(\pi, \pi)$  points. In the calculated spectrum we also notice two cusps near  $\mathbf{k} = (\pi/2, 0)$  and  $\mathbf{k} = (\pi, \pi/2)$  which are absent in the experimental spectrum. This discrepancy may be attributed to the fact that to this high-intensity patch which looks like a single band in the plot, actually contribute two of many bands which may be seen in Fig.6. The band which appears in the results of the exact diagonalization performed for the  $tJM$  and the results of the calculation based on the scenario of the columnar spin-Peierls order [31] has also the strong dispersion but does not flatten in the anti-nodal region. Despite that neither the spectral weight of the quasiparticle propagating in the bond ordered spin background nor the spectral weight of the quasiparticle propagating in the AF background [43] resembles ARPES spectra from doped LSCO and doped Nd-LSCO in the stripe phase, spectral properties of the model in which these two phases coexist gives rise to qualitative agreement with experimental data. This agreement may be attributed to the fact that the band structure of the model of nano-scale phase separation which we discuss here has some features which are present in band structures of both pure homogeneous phases. For example in our results we actually see a remnant of a strip formed by high intensity which takes the shape of a strongly dispersing band along the line between points  $(0, 0)$  and  $(\pi, 0)/(0, \pi)$  and resembles the band that is formed in

the columnar bond-ordered phase. This band-like structure actually does not flatten and reaches the maximum near the points  $(0, \pi/2)/(\pi/2, 0)$ . On the other hand it is likely that the presence of this maximum may be attributed to the brute force method of sewing the bond-ordered parts of the system with the parts which are AF-ally ordered. One thing is for sure, that the lack of the straight high intensity patch at the anti-nodal region in results of the theory based on the scenario of the columnar spin-Peierls phase demonstrates that the spectral function calculated within this picture does not agree in some details with measured ARPES spectra and suggests that it is necessary to take into account also the long range AF correlations in order to formulate a theory which accounts for the spectral properties of the cuprates in the stripe phase. In the region between the zone center and antinodal points  $(\pi, 0)/(0, \pi)$  similar agreement has been observed between the experimental data and results of a calculation based on the dynamical mean field theory (DMFT) applied to the Hubbard model [17].

Along the line connecting the points  $(0, 0)$  and  $(\pi, \pi)$  both in ARPES spectra and in our results we see a band in the vicinity of the Fermi surface. This band has a maximum at the points  $(\pi/2, \pi/2)$ , bends downward and disappears near the zone corner. A similar feature may be observed in the results of an exact diagonalization performed for the  $t-t'-t''-J$  model and in the results of the calculation performed within the scenario of the bond-ordered columnar phase [31]. The DMFT of the stripe phase in the Hubbard model at the doping level 15% gives rise to a slightly different result, namely it seems that the band crosses the Fermi level near the point  $(\pi/2, \pi/2)$ .

The intensity map of the one-electron removal spectral function  $A^-(\mathbf{k}, \omega)$  at the Fermi energy obtained in the framework of the scenario which assumes coexistence of bond and AF orders is depicted by Fig.8. Fig.8(a) refers to results of the calculation in which we have assumed that bond order is formed on legs in ladder-like DWs. That figure also shows some agreement with ARPES data from LSCO and Nd-LSCO [13] obtained for the doping level 15%. We see well developed spectral weight in the nodal regions. These regions are bridged by high-intensity continuous almost straight high-intensity patches. It seems that the agreement between the experimental results and the results of the theory based on the mixture of the bond formalism and the spin polaron approach is better in this respect than the agreement with results of previous calculations based on the CPT applied to microscopic models which are the  $tJM$  and the Hubbard model [20, 25].

Fig.8(b) depicts the spectral weight at the Fermi energy obtained in a separate calculation for the underlying spin background with bond order on rungs. We know from the results of a previous paper [33] that such a structure is less stable and do not expect much similarity with experimental results. Such a lack of similarity may be seen, indeed. For example the high-intensity patches does not form a shape resembling the Fermi sur-

face obtained by means of calculations based on the local density approach. Such a shape may be observed both in experimental spectra and in Fig.8(a). In Fig.8 apart from patches of high spectral density we notice additional regular structures formed by regions of enhanced intensity. It seems that the origin of those structures may be attributed to simplicity of our approach within which fluctuations of the underlying spin structure depicted in Fig.1 are neglected to a great extent. It is natural to expect that such fluctuations smear out the contribution to the spectral function from excitations which may be classified as incoherent background and only the dominating quasiparticle contributions, which may be seen as bright patches in Fig.8, are preserved in the real system.

Calculations based on the phenomenological approach to disordered charge stripes and antiphase spin domains give rise to a pattern formed by regions of high spectral intensity in the 1BZ which strongly resembles ARPES spectra [24, 28]. Unfortunately no microscopic justification has been provided, of phenomenological one-body Hamiltonians which has been applied to derive the spectral density by means of calculations based on this scenario. Our calculation is based on the microscopic  $t$ - $t'$ - $t''$ - $J$  model. On the other hand it seems that disorder may give rise spreading of spectral weight over the whole anti-nodal region. Such a spreading is not observed in the results of our calculation. In a previous paper we have demonstrated that the magnetic structure of the stripe which we have considered here, is likely to have lowest energy at and above the doping level 12.5%, if the distance between axes of nearest stripes is 4 lattice spacings, as it has been suggested by experiments [33]. Bond order parallel to stripe axes and long range AF order coexist in this magnetic structure. It has been suggested that the shape of the Fermi surface seen in ARPES spectra from Nd-LSCO and LSCO at the doping level in the range 12.5% – 15% may be also explained in the framework of more conventional band calculations which neglect the formation of nano-scale inhomogeneities [44]. It seems to be hard to reconcile such a way of thinking with the evidence for stripes forming in these systems.

In conclusion, motivated by results of a previous calculation [33] indicating that, at the doping level 1/8 and above, the stripe structure, which consists of a) hole-filled two-leg ladder-like DWs with the spin-Peierls order formed on legs and b) AF domains of width 2 lattice spacings and with the changing phase of the sublattice magnetization by  $\pi$  across each DW, is stable, we have performed the calculation of the single-particle spectral density which is generated in such a system. Our analysis

has been made in the framework of the  $t$ - $t'$ - $t''$ - $J$  model, with parameter values in the range suggested by comparison between band structure calculations and the Fermi surface of overdoped LSCO systems. The calculation which we have performed is a combination of the bond fermion method and the spin polaron approach. We observe pronounced spectral weight both in the anti-nodal and nodal regions. Very similar features may be seen in ARPES spectra from LSCO and Nd-LSCO at the filling level 15%, which is exactly the same as we have assumed in the calculation. This similarity is not trivial, because different optional structures of bond order in DWs, as the spin-Peierls order on rungs in the ladder-like DWs or the bond order which takes the shape of two layers in a brick-wall, give rise to spectra at the Fermi level which have completely different forms. We consider the observed agreement between experiment and theory as an argument for the scenario of coexisting bond and long range AF orders in the stripe phase of doped cuprates.

### Acknowledgments

PW acknowledges partial support by the Polish Science Committee (KBN) under contract No 2P03B00925.

### APPENDIX

We list here contributions to matrix elements (39). The contribution to (39) is  $\alpha_0$  for the following values of indices  $(i', j')$ ,  $(n, l)$ ,  $(i, j)$ :  $(2, 1)$ ,  $(0, 0)$ ,  $(2, 1)$ ;  $(3, 0)$ ,  $(0, 0)$ ,  $(3, 0)$ ;  $(4, 0)$ ,  $(0, 0)$ ,  $(4, 0)$ ;  $(5, 1)$ ,  $(0, 0)$ ,  $(5, 1)$ . The contribution is  $-\frac{1}{\sqrt{2}}$  for  $(0, 0)$ ,  $(0, 0)$ ,  $(0, 0)$ ;  $(0, 1)$ ,  $(0, 0)$ ,  $(0, 1)$ ;  $(1, 0)$ ,  $(0, 0)$ ,  $(1, 0)$ ;  $(1, 1)$ ,  $(0, 0)$ ,  $(1, 1)$ ;  $(4, 0)$ ,  $(0, 0)$ ,  $(4, 0)$ ;  $(4, 1)$ ,  $(0, 0)$ ,  $(4, 1)$ ;  $(5, 0)$ ,  $(0, 0)$ ,  $(5, 0)$ ;  $(5, 1)$ ,  $(0, 0)$ ,  $(5, 1)$ ;  $-\frac{1}{2\sqrt{2}}$  for  $(0, 0)$ ,  $(0, 0)$ ,  $(0, 0)$ ;  $(1, 0)$ ,  $(0, 0)$ ,  $(1, 0)$ ;  $(4, 1)$ ,  $(0, 0)$ ,  $(4, 1)$ ;  $(5, 1)$ ,  $(0, 0)$ ,  $(5, 1)$ ;  $\frac{1}{2\sqrt{2}}$  for  $(0, 1)$ ,  $(0, 0)$ ,  $(0, 1)$ ;  $(1, 1)$ ,  $(0, 0)$ ,  $(1, 1)$ ;  $(4, 0)$ ,  $(0, 0)$ ,  $(4, 0)$ ;  $(5, 0)$ ,  $(0, 0)$ ,  $(5, 0)$ ;  $-\frac{\alpha_1}{4}$  for  $(2, 0)$ ,  $(0, 0)$ ,  $(2, 1)$ ;  $(2, 0)$ ,  $(0, 0)$ ,  $(3, 0)$ ;  $(2, 0)$ ,  $(0, -1)$ ,  $(2, 1)$ ;  $(3, 1)$ ,  $(0, 0)$ ,  $(2, 1)$ ;  $(3, 1)$ ,  $(0, 0)$ ,  $(3, 0)$ ;  $(3, 0)$ ,  $(0, 0)$ ,  $(6, 0)$ ;  $(6, 1)$ ,  $(0, 0)$ ,  $(7, 1)$ ;  $(6, 1)$ ,  $(0, 1)$ ,  $(6, 0)$ ;  $(7, 0)$ ,  $(0, 0)$ ,  $(6, 0)$ ;  $(7, 0)$ ,  $(0, 0)$ ,  $(7, 1)$ ;  $(7, 0)$ ,  $(0, -1)$ ,  $(7, 1)$ ;  $-\frac{\alpha_2}{2}$  for  $(2, 1)$ ,  $(0, 0)$ ,  $(3, 0)$ ;  $(2, 1)$ ,  $(0, 1)$ ,  $(3, 0)$ ;  $(3, 0)$ ,  $(0, 0)$ ,  $(2, 1)$ ;  $(3, 0)$ ,  $(0, -1)$ ,  $(2, 1)$ ;  $(2, 1)$ ,  $(0, 1)$ ,  $(2, 1)$ ;  $(6, 0)$ ,  $(0, 0)$ ,  $(7, 1)$ ;  $(6, 0)$ ,  $(0, -1)$ ,  $(7, 1)$ ;  $(7, 1)$ ,  $(0, 0)$ ,  $(6, 0)$ ;  $(7, 1)$ ,  $(0, 1)$ ,  $(6, 0)$ ;  $-\frac{\alpha_2}{4}$  for  $(2, 1)$ ,  $(0, 1)$ ,  $(2, 1)$ ;  $(2, 1)$ ,  $(0, -1)$ ,  $(2, 1)$ ;  $(3, 0)$ ,  $(0, 1)$ ,  $(3, 0)$ ;  $(3, 0)$ ,  $(0, -1)$ ,  $(3, 0)$ ;  $(6, 0)$ ,  $(0, 1)$ ,  $(6, 0)$ ;  $(6, 0)$ ,  $(0, -1)$ ,  $(6, 0)$ ;  $(7, 1)$ ,  $(0, 1)$ ,  $(7, 1)$ ;  $(7, 1)$ ,  $(0, -1)$ ,  $(7, 1)$ .

---

[1] T. R. Thurston, R. J. Birgeneau, M. A. Kastner, N. W. Preyer, G. Shirane, Y. Fujii, K. Yamada, Y. Endoh, K. Kakuri, M. Matsuda, Y. Hidaka, and T. Murakami, Phys. Rev. B **40**, 4585 (1989); S.-W. Cheong, G. Aeppli, T. E. Mason, H. Mook, S. M. Hyden, P. C. Canfield, Z. Fisk,

K. N. Clausen, and J. L. Martinez, Phys. Rev. Lett. **67**, 1791 (1991); T. R. Thurston, P. M. Gehring, G. Shirane, R. J. Birgeneau, M. A. Kastner, Y. Endoh, M. Matsuda, K. Yamada, K. Kojima, and I. Tanaka, Phys. Rev. B **46**, 9128 (1992).

[2] J. M. Tranquada, B. J. Sternlieb, J. D. Axe, Y. Nakamura, S. Uchida, *Nature* **375**, 561 (1995).

[3] M. Matsuda, R. J. Birgeneau, H. Chou, Y. Endoh, M. A. Kastner, H. Kojima, K. Kuroda, G. Shirane, I. Tanaka, and K. Yamada, *J. Phys. Soc. Jpn.* **62**, 443 (1993); K. Yamada, S. Wakimoto, G. Shirane, C. H. Lee, M. A. Kastner, S. Hosoya, M. Greven, Y. Endoh, and R. J. Birgeneau, *Phys. Rev. Lett.* **75**, 1626 (1995); K. Hirota, K. Yamada, I. Tanaka, and H. Kojima, *Physica B* **241-243**, 817 (1998); H. Kimura, et al, *Phys. Rev. B* **59**, 6517 (1999); J. M. Tranquada, N. Ichikawa, K. Kakurai, and S. Uchida, *J. Phys. Chem. Solids* **60**, 1019 (1999); J. M. Tranquada, N. Ichikawa, and S. Uchida, *Phys. Rev. B* **59**, 14712 (1999).

[4] S. A. Kivelson, I. P. Bindloss, E. Fradkin, V. Oganesyan, J. M. Tranquada, A. Kapitulnik, and C. Howald, *Rev. Mod. Phys.* **75**, 1201 (2003).

[5] Y. Ando, K. Segawa, S. Komiya, and A. N. Lavrov, *Phys. Rev. Lett.* **88**, 137005 (2002).

[6] C. Hess, B. Büchner, M. Hücker, R. Gross, and S-W. Cheong, *Phys. Rev. B* **59**, 10397 (1999).

[7] A. W. Hunt, P. M. Singer, K. R. Thurber, and T. Imai, *Phys. Rev. Lett.* **82**, 4300 (1999); M.-H. Julien, F. Borsa, P. Carreta, M. Horvatić, C. Berthier, and C. T. Lin, *Phys. Rev. Lett.* **83**, 604 (1999); P. M. Singer, A. W. Hunt, A. F. Cederström, and T. Imai, *Phys. Rev. B* **60**, 15345 (1999); B. J. Suh, P. C. Hammel, M. Hücker, and B. Büchner, *Phys. Rev. B* **59**, R3952 (1999); N. J. Curro, P. C. Hammel, B. J. Suh, M. Hücker, B. Büchner, A. Ammerahl, and A. Revcolevschi, *Phys. Rev. Lett.* **85**, 642 (2000); B. J. Suh, P. C. Hammel, M. Hücker, B. Büchner, U. Ammerahl, and A. Revcolevschi, *Phys. Rev. B* **61**, R9265 (2000); G. B. Teitelbaum, B. Büchner, and H. de Gronckel, *Phys. Rev. Lett.* **84**, 2949 (2000), A. W. Hunt, P. M. Singer, A. F. Cederström, and T. Imai, *Phys. Rev. B* **64**, 134525 (2001); H.-H. Julien, A. Campana, A. Rigamonti, P. Carretta, F. Borsa, P. Kuhns, A. P. Reyes, W. G. Moulton, M. Horvatić, C. Berthier, A. Vietkin, and A. Revcolevschi, *Phys. Rev. B* **63**, 144508 (2001); G. B. Teitelbaum, I. M. Abu-Shiekah, O. Bakharev, H. B. Brom, and J. Zaanen, *Phys. Rev. B* **63**, 020507 (2001); B. Simović, P. C. Hammel, M. Hücker, B. Büchner, and A. Revcolevschi, *Phys. Rev. B* **68**, 012415 (2003).

[8] E. S. Božin, G. H. Kwei, H. Takagi, and S. J. L. Billinge, *Phys. Rev. Lett.* **84**, 5856 (2000).

[9] M. Braden, M. Meven, W. Reichardt, L. Pintschovius, M. T. Fernandez-Diaz, G. Heger, F. Nakamura, and T. Fujita, *Phys. Rev. B* **63**, 140510 (2001).

[10] A. Bianconi, N. L. Saini, A. Lanzara, M. Missori, T. R. H. Oyanagi, H. Yamaguchi, K. Oka, and T. Ito, *Phys. Rev. Lett.* **76**, 3412 (1996); A. Lanzara, N. L. Saini, T. Rossetti, A. Bianconi, H. Oyanagi, H. Yamaguchi, and Y. Maeno, *Solid. State Commun.* **97**, 93 (1996); N. L. Saini, A. Lanzara, H. Oyanagi, H. Yamaguchi, K. Oka, T. Ito, and A. Bianconi, *Phys. Rev. B* **55**, 12759 (1997).

[11] A. V. Fedorov, T. Valla, P. D. Johnson, Q. Li, G. D. Gu, and N. Koshizuka, *Phys. Rev. Lett.* **82**, 2179 (1999); A. Ino, C. Kim, T. Mizokawa, Z. X. Shen, A. Fujimori, M. Takaba, K. Tamasaku, H. Eisaki, and S. Uchida, *J. Phys. Soc. Jpn.* **68**, 1496 (1999); T. Valla, A. V. Fedorov, P. D. Johnson, B. O. Wells, S. L. Hulbert, Q. Li, G. D. Gu, and N. Koshizuka, *Science* **285**, 2110 (1999); P. J. White, Z. X. Shen, D. L. Feng, C. Kim, M. Z. Hasan, J. M. Harris, A. G. Loeser, H. Ikeda, R. Yoshikazi, G. D. Gu, and N. Koshizuka, preprint cond-mat/9901349.

[12] X. J. Zhou, P. Bogdanov, S. A. Kellar, T. Noda, H. Eisaki, S. Uchida, Z. Hussain, Z.-X. Shen, *Science* **286**, 268 (1999).

[13] X. J. Zhou, T. Yoshida, S. A. Kellar, P. V. Bogdanov, E. D. Lu, A. Lanzara, M. Nakamura, T. Noda, T. Kakeshita, H. Eisaki, S. Uchida, A. Fujimori, et al., *Phys. Rev. Lett.* **86**, 5578 (2001).

[14] J. C. Campuzano, M. R. Norman, and M. Randeria, in *Physic of Conventional and Unconventional Superconductors*, edited by K. H. Bennemann, and J. B. Ketterson (Springer, Berlin, 2003).

[15] A. Damascelli, A. Z. Hussain, and Z.-X. Shen, *Rev. Mod. Phys.* **75**, 473 (2003).

[16] M. Ichioka, and K. Machida, *J. Phys. Soc. Jpn.* **68**, 4020 (1999).

[17] M. Fleck, A.I. Lichtenstein, E. Pavarini, and A. M. Oleś, *Phys. Rev. Lett.* **84**, 4962 (2000); M. Fleck, A.I. Lichtenstein, and A. M. Oleś, *Phys. Rev. B* **64**, 134528 (2001).

[18] R. S. Markiewicz, *Phys. Rev. B* **62**, 1252 (2000); P. Wróbel, and R. Eder, *Phys. Rev. B* **62**, 4048 (2000).

[19] P. Wróbel, and R. Eder, *Int. Jour. Mod. Phys. B* **14**, 3759 (2000).

[20] M. G. Zacher, R. Eder, E. E. Arrigoni, and W. Hanke, *Phys. Rev. Lett.* **85**, 2585 (2000).

[21] E. W. Carlson, D. Orgad, S. A. Kivelson, and V. J. Emery, *Phys. Rev. B* **62**, 3422 (2001).

[22] J. Eroles, G. Ortiz, A. V. Balatsky, and A. R. Bishop, *Phys. Rev. B* **64**, 174510 (2001).

[23] M. Granath, V. Oganesyan, S. A. Kivelson, E. Fradkin, and V. J. Emery, *Phys. Rev. Lett.* **87**, 167011 (2001); G.-H. Gweon, J. D. Denlinger, J. W. Allen, R. Claesson, C. G. Olson, H. Hoechst, J. Marcus, C. Schlenker, and L. F. Schneemeyer, *J. Electron Spectrosc. Relat. Phenom.* **117-118**, 481 (2001); D. Orgad, S. A. Kivelson, E. W. Carlson, V. J. Emery, X. J. Zhou, and Z. X. Shen, *Phys. Rev. Lett.* **86**, 4362 (2001).

[24] M. Granath, V. Oganesyan, D. Orgad, and S. A. Kivelson, *Phys. Rev. B* **65**, 184501 (2002).

[25] M. G. Zacher, R. Eder, E. E. Arrigoni, and W. Hanke, *Phys. Rev. B* **65**, 045109 (2002).

[26] E. W. Carlson, V. J. Emery, S. A. Kivelson, and D. Orgad, in *The Physics of Conventional and Unconventional Superconductors*, edited by K. H. Bennemann, and J. B. Ketterson (Springer, Berlin, 2003); M. Granath, preprint cond-mat/0401063.

[27] A. Ino, C. Kim, M. Nakamura, T. Yoshida, T. Mizokawa, A. Fujimori, T. Kakeshita, H. Eisaki, and S. Uchida, *Phys. Rev. B* **62**, 4137 (2000).

[28] M. I. Salkola, V. J. Emery, and S. A. Kivelson, *Phys. Rev. Lett.* **77**, 155 (1996).

[29] P.W. Anderson, *Science* **235**, 1196 (1987); D. S. Rokshar, and S. A. Kivelson, *Phys. Rev. Lett.* **61**, 2376 (1988); T. Dombre, and G. Kotliar, *Phys. Rev. B* **39**, 855 (1989); E. Fradkin, and S. A. Kivelson, *Mod. Phys. Lett. B* **4**, 225 (1990); N. Read, and S. Sachdev, *Phys. Rev. B* **42**, 4568 (1990); S. Sachdev, and N. Read, *Phys. Rev. Lett.* **77**, 4800 (1996); N. Read, and S. Sachdev, *Nucl. Phys. B* **316**, 609 (1998); M. Vojta, and S. Sachdev, *Phys. Rev. Lett.* **83**, 3916 (1999); E. Altman, and A. Auerbach, *Phys. Rev. B* **65**, 104508 (2002); S. Sachdev, and K. Park, *Ann. Phys. (N.Y.)* **298**, 58 (2002); M. Vojta, *Phys. Rev. B* **66**, 104505 (2002); S. Sachdev, *Rev. Mod. Phys.* **75**, 913 (2003).

[30] R. Eder, and Y. Ohta, Phys. Rev. B **69**, 094433 (2004).

[31] R. Eder, and Y. Ohta, Phys. Rev. B **69**, 100502(R) (2004).

[32] S. M Hayden, H. A. Mook, P. Dai, T. G. Perring, and F. Dogan, Nature **429**, 531 (2004); J. M. Tranquada, H. Woo, T. G. Perring, H. Goka, G. D. Gu, G. Xu, M. Fujita, and K. Yamada, Nature **429**, 534 (2004).

[33] P. Wróbel, A. Maciąg, and R. Eder, preprint cond-mat/0408578.

[34] A. L. Chernyshev, A. H. Castro Neto, and A. R. Bishop, Phys. Rev. Lett. **84**, 4922 (2000); A. L. Chernyshev, S.R. White, and A. H. Castro Neto, Phys. Rev. B **65**, 214527 (2002).

[35] K. W. Becker, R. Eder, and H. Won, Phys. Rev. B **45**, 4864 (1992).

[36] R. Eder, Phys. Rev. B **57**, 12832 (1998).

[37] C. Jurecka and W. Brenig Phys. Rev. B **61**, 14307 (2000); W. Brenig, and K. W. Becker, Phys. Rev. B **64**, 214413 (2001); C. Hess, C. Baumann, U. Ammerahl, B. Büchner, F. Heidrich-Meisner, W. Brenig, and A. Revcolevschi, Phys. Rev. B **64**, 184305 (2001); C. Jurecka, and W. Brenig, Phys. Rev. B **63**, 094409 (2001); F. Heidrich-Meisner, A. Honecker, D. C. Cabra, and W. Brenig, Phys. Rev. B **68**, 134436 (2003).

[38] A.L. Chernyshev, and R.F. Wood, in *Models and Methods of High-Tc Superconductivity: Some Frontal Aspects*, vol. 1, edited by J. K. Srivastava and S. M. Rao (Nova Science Publishers, Inc., Hauppauge NY, 2003); and references therein.

[39] L.N. Bulaevskii, E.L. Nagaev, and D.I. Khomskii, Zh. Eksp. Teor. Fiz. **54**, 1562 (1968); W. F. Brinkman and T. M. Rice, Phys. Rev. B **2**, 1324 (1970); C. L. Kane, P. A. Lee, and N. Read, Phys. Rev. B **39**, 6880 (1988); F. Marsiglio, A. E. Ruckenstein, S. Schmitt-Rink, and C. M. Varma, Phys. Rev. B **43** 10882 (1991); S. Schmitt-Rink, C. M. Varma, and A. E. Ruckenstein, Phys. Rev. Lett. **60**, 2793 (1988); B. Shraiman, and E. Siggia, Phys. Rev. Lett. **60**, 740 (1988); S. Trugman, Phys. Rev. B **37**, 1597 (1988), **41**, 892 (1990); see also J. R. Schrieffer, X.-G. Wen, and S.-C. Zhang, Phys. Rev. Lett. **60**, 944 (1988); P. Béran, D. Poilblanc, and R.B. Laughlin, Nucl. Phys. B **473**, 707 (1996); R. B. Laughlin, Phys. Rev. Lett. **79**, 1726 (1997).

[40] A. Ino, C. Kim, M. Nakamura, T. Yoshida, T. Mizokawa, A. Fujimori, Z.-X. Shen, T. Kakeshita, H. Eisaki, and S. Uchida, Phys. Rev. B **65**, 094504 (2002).

[41] R. Eder, and K. W. Becker, Phys. Rev. B **44**, 6982 (1991); R. Eder and K. W. Becker, Z. Phys. B **78**, 219 (1990); R. Eder, K. W. Becker and W. Stephan, Z. Phys. B **81**, 33 (1990).

[42] T. Tohyama, S. Nagai, Y. Shibata, and S. Maekawa, Phys. Rev. Lett. **82**, 4910 (1999); T. Tohyama, S. Maekawa, Supercond. Sci. Technol. **13**, R17 (2000).

[43] B. O. Wells, Z.-X. Shen, A. Matsuda, D. M. King, M. A. Kastner, M. Greven, and R. J. Birgeneau, Phys. Rev. Lett. **74**, 964 (1995)

[44] A. Bansil and R.S. Markiewicz (private communication).

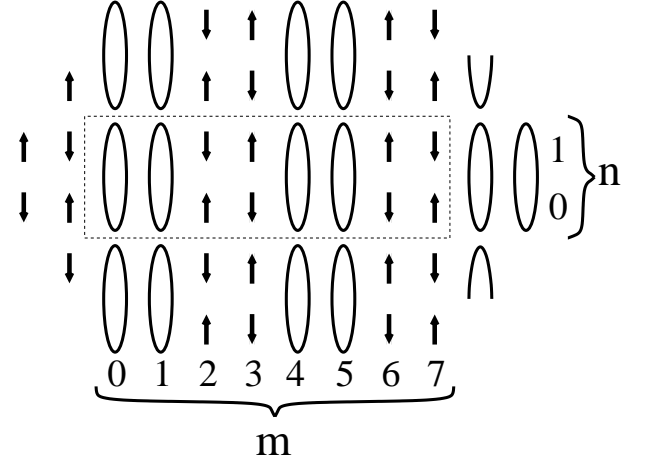


FIG. 1: Elementary cell of the underlying spin structure assumed in the calculation (inside the dashed rectangle). Ovals represent singlets.

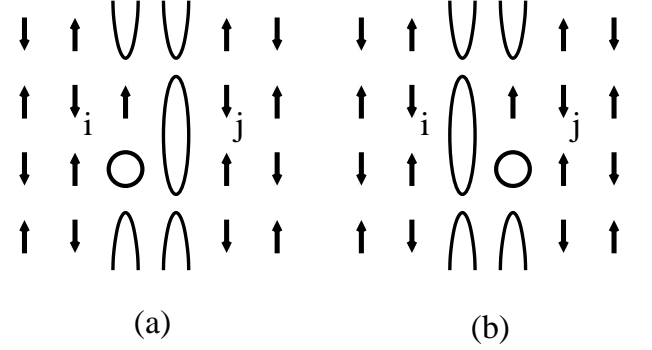


FIG. 2: The mechanism which gives rise to FM coupling between nearest spins which belong to different domains. Notice, that these spins would belong to the same AF sublattice if the system were homogeneously ordered.

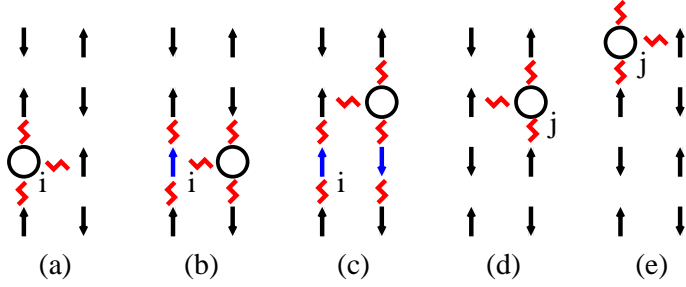


FIG. 3: Graphical representation of some states involved in the process of hole propagation inside an AF domain. Zig-zag lines represent “broken bonds” contribution from which to Ising energy is higher by  $J/2$  than contribution from bonds occupied by two antiparallel spins.

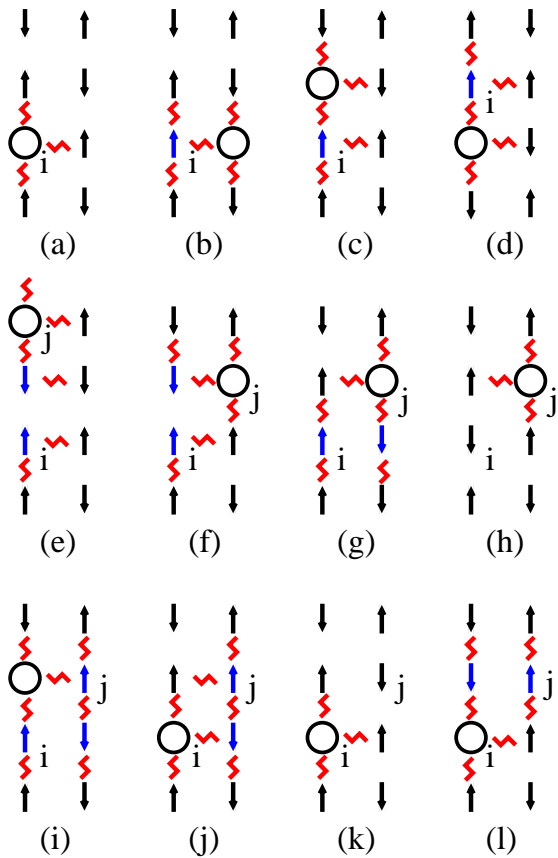


FIG. 4: Illustration of processes contributing to some terms in the effective Hamiltonian. These terms define the on-site energy and the quasiparticle hopping between sites which belong to AF domains.

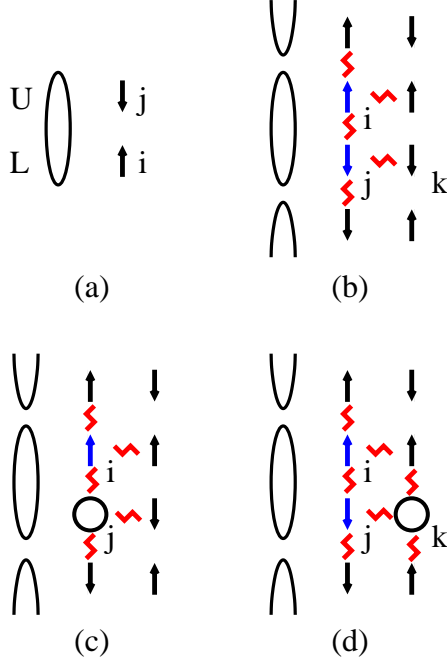


FIG. 5: Graphical representation of states involved in generation of quantum fluctuations in  $|\Omega\rangle$ . Contributions from these fluctuations determine to a large extent the shape of the spectral function.

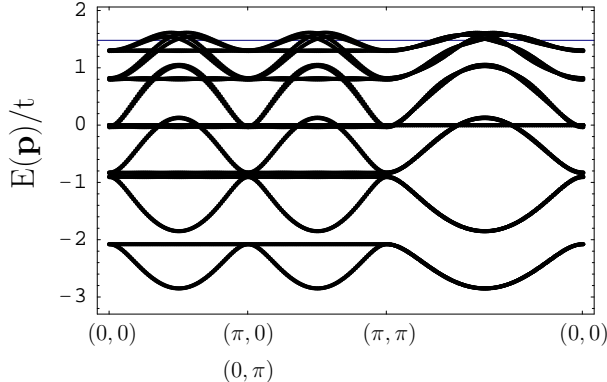


FIG. 6: Band structure in the stripe phase, obtained within the scenario of coexisting bond and AF orders.

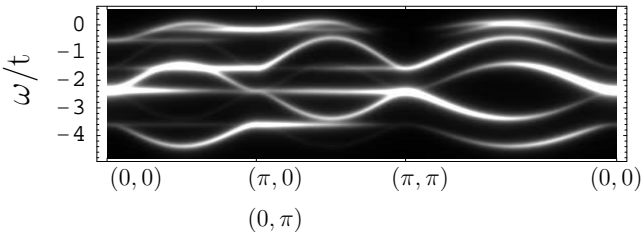


FIG. 7: Spectral weight intensity  $A^-(\mathbf{k}, \omega)$  along some directions at the doping level 15%. Lorentzian broadening with the width  $0.1t$  has been applied.

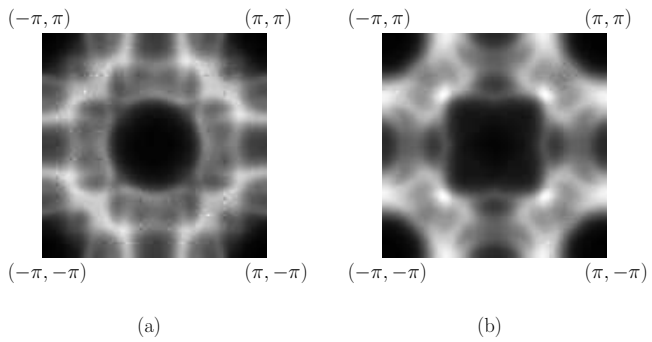


FIG. 8: Intensity map of the spectral weight  $A^-({\mathbf k}, \omega)$  at  $E_F$ .